openheart

Relationship of age, atherosclerosis and angiographic stenosis using artificial intelligence

Rebecca Jonas ,[1] James Earls,[2] Hugo Marques,[3] Hyuk-Jae Chang,[4] Jung Hyun Choi,[5] Joon-Hyung Doh,[6] Ae-Young Her,[7] Bon Kwon Koo,[8] Chang-Wook Nam,[9] Hyung-Bok Park,[10] Sanghoon Shin,[11] Jason Cole,[12] Alessia Gimelli,[13] Muhammad Akram Khan,[14] Bin Lu,[15] Yang Gao,[16] Faisal Nabi,[17] Ryo Nakazato,[18] U Joseph Schoepf,[19] Roel S Driessen,[20] Michiel J Bom,[21] Randall C Thompson,[22] James J Jang,[23] Michael Ridner,[24] Chris Rowan,[25] Erick Avelar,[26] Philippe Généreux,[27] Paul Knaapen,[28] Guus A de Waard ,[28] Gianluca Pontone,[29] Daniele Andreini,[29] Mouaz H Al-Mallah,[30] Robert Jennings,[2] Tami R Crabtree,[2] Todd C Villines,[31] James K Min,[2] Andrew D Choi[32]

► Additional supplemental material is published online only. To view, please visit the journal online (http://dx.doi.org/10.1136/openhrt-2021-001832).

To cite: Jonas R, Earls J, Marques H, *et al*. Relationship of age, atherosclerosis and angiographic stenosis using artificial intelligence. *Open Heart* 2021;**8**:e001832. doi:10.1136/openhrt-2021-001832

Received 31 August 2021
Accepted 8 October 2021

For numbered affiliations see end of article.

Correspondence to
Dr Andrew D Choi; adchoi@mfa.gwu.edu

ABSTRACT

Objective The study evaluates the relationship of coronary stenosis, atherosclerotic plaque characteristics (APCs) and age using artificial intelligence enabled quantitative coronary computed tomographic angiography (AI-QCT).

Methods This is a post-hoc analysis of data from 303 subjects enrolled in the CREDENCE (Computed TomogRaphic Evaluation of Atherosclerotic Determinants of Myocardial IsChEmia) trial who were referred for invasive coronary angiography and subsequently underwent coronary computed tomographic angiography (CCTA). In this study, a blinded core laboratory analysing quantitative coronary angiography images classified lesions as obstructive (≥50%) or non-obstructive (<50%) while AI software quantified APCs including plaque volume (PV), low-density non-calcified plaque (LD-NCP), non-calcified plaque (NCP), calcified plaque (CP), lesion length on a per-patient and per-lesion basis based on CCTA imaging. Plaque measurements were normalised for vessel volume and reported as % percent atheroma volume (%PAV) for all relevant plaque components. Data were subsequently stratified by age <65 and ≥65 years.

Results The cohort was 64.4±10.2 years and 29% women. Overall, patients >65 had more PV and CP than patients <65. On a lesion level, patients >65 had more CP than younger patients in both obstructive (29.2 mm^3 vs 48.2 mm^3; p<0.04) and non-obstructive lesions (22.1 mm^3 vs 49.4 mm^3; p<0.004) while younger patients had more %PAV (LD-NCP) (1.5% vs 0.7%; p<0.038). Younger patients had more PV, LD-NCP, NCP and lesion lengths in obstructive compared with non-obstructive lesions. There were no differences observed between lesion types in older patients.

Conclusion AI-QCT identifies a unique APC signature that differs by age and degree of stenosis and provides a foundation for AI-guided age-based approaches to atherosclerosis identification, prevention and treatment.

Key questions

What is already known about this subject?

► High-risk atherosclerotic plaque characteristics put patients at risk for cardiovascular events, but is challenging for clinical practice using currently available methods.

What does this study add?

► This study provides a lesion-based assessment of plaque changes by age.
► This study provides support for use of artificial intelligence enabled quantitative coronary computed tomographic angiography (AI-QCT) to identify an age associated plaque phenotype.

How might this impact on clinical practice?

► These findings provide clinicians with an opportunity to tailor patient treatment based on the risk associated with a patient's plaque profile.
► These findings provide a basis for evaluating patients for enhanced prevention based on age with AI-QCT.

INTRODUCTION

Coronary computed tomographic angiography (CCTA) has been validated as a non-invasive imaging modality capable of both ruling out coronary artery disease (CAD) and quantifying coronary plaque.[1 2] Advancements in the diagnostic specificity of CCTA have allowed not only for quantification of total plaque through the entirety of coronary vascular anatomy, but also for the specific identification and quantification of various plaque characteristics in stable and unstable lesions.[3] This capability along with the use of artificial intelligence (AI) and machine

learning have resulted in an expanding foundation of data describing high risk atherosclerotic plaque characteristics (APCs) that put specific patient populations at increased risk for major adverse cardiovascular events (MACE).[4] Several APCs, namely, total plaque volume (PV), low density non-calcified plaque (LD-NCP), non-calcified plaque (NCP), calcified plaque (CP) and lesion length have been identified as significant quantifiable characteristics with prognostic value.[5 6] The per cent atheroma volume (PAV) reflects each APC's quantity after normalising for vessel volume and has been suggested as a way of calculating and reporting APCs. Other significant quantifiable markers included vascular positive remodelling (PR), spotty calcification (SC), napkin-ring sign and high-risk plaque (HRP), defined as coronary lesions with both LD-NCP and PR.[5 7–9] There have been distinct differences in the characteristics of these plaques based on various demographic and clinical variables, but whether these characteristics vary by age is still being investigated. This study intended to identify whether obstructive and non-obstructive lesions have different plaque characteristics based on age, specifically in individuals older than 65 compared with those younger than 65 years through plaque quantification using AI enabled quantitative coronary computed tomographic angiography (AI-QCT).

METHODS

The study population was comprised of the derivation cohort of the Computed TomogRaphic Evaluation of Atherosclerotic Determinants of Myocardial IsChEmia (CREDENCE) trial (ClinicalTrials.gov, NCT02173275), which was a prospective, multicentre diagnostic derivation–validation controlled clinical trial recruiting stable patients from 2014 to 2017. Sites and Investigators are listed in online supplemental appendix A. A detailed design manuscript was previously published.[10] Enrolled patients underwent CCTA followed by invasive quantitative coronary angiography as the reference test within 60 days. Eligibility criteria included referral to non-emergent invasive coronary angiography (ICA) based on the American College of Cardiology/American Heart Association clinical practice guidelines for stable ischaemic heart disease. All index tests were interpreted in blinded fashion by an imaging core laboratory. Patient demographics, cardiovascular risk factors, laboratory values and medications were prospectively collected and recorded at the time of baseline and follow-up CCTAs.

CCTA imaging protocols

CCTA was performed using single or dual source CT scanners of ≥64-detector rows. Sites performed CCTA in accordance with the guidelines established by the Society of Cardiovascular Computed Tomography (SCCT).[11] Nitroglycerin was administered immediately prior to CCTA to enhance imaging quality. Image quality for CCTA was acceptable in 99% of patients.

AI enabled quantification of CCTA

The AI-based approach to CCTA interpretation in this study was performed using a validated and US Food and Drug Administration (FDA)-cleared software service (Cleerly Inc, New York, New York) that performs automated analysis of CCTA using a series of validated convolutional neural network models (including VGG19 network, 3D U-Net and VGG Network Variant) for image quality assessment, coronary segmentation and labelling, lumen wall evaluation and vessel contour determination and plaque characterisation.[12 13] The centerline algorithm was developed from 1 007 945 images, which comprised 23 068 vessels from 3671 patients (online supplemental appendix B). The lumen and vessel wall algorithms were developed from 1 414 877 images, which comprised 8555 vessels from 3676 patients. First, the AI-aided approach produces a centerline along each coronary artery, and then for lumen and outer vessel wall contouring. This is applied to each phase of the examination and the two optimal series are identified for further analysis. After establishing vessel wall contours, distance and volumetric analyses were performed based on specified Hounsfield unit (HU) cut offs for characterising plaque characteristics. After the AI algorithm has finished all operations, as mandated by the FDA, a quality control cardiac CT trained technician reviews the results of the AI analysis in all cases with manual adjustment if necessary.

Coronary segments with a diameter ≥2 mm were included in the analysis using the modified 18-segment SCCT model.[14] Each segment was evaluated for the presence or absence of coronary atherosclerosis, defined as any tissue structure >1 mm^2 within the coronary artery wall that was differentiated from the surrounding epicardial tissue, epicardial fat or the vessel lumen itself. The following APCs were evaluated:

- Atherosclerosis: Quantitative atherosclerosis characterisation was performed for every coronary artery and its branches using the automated AI-enabled web-based software platform (Cleerly Labs).[13] PVs (mm^3) were calculated for each coronary lesion and then summated to compute the PV at the patient level. Plaque with a minimum volume of ≥3 mm^3 was included for analysis. This provided data for analysis on both the lesion and patient level. PV was further categorised using HU ranges with NCP defined as 30–350 HU; LD-NCP defined as plaques <30 HU; and CP defined as >350 HU. Coronary plaque burden was normalised to vessel volume to account for natural variation in coronary artery volume. Plaque burden was reported as PAV, CP PAV, NCP PAV and LD-NCP PAV which was calculated as PV (by each aforementioned type)/vessel volume×100%. Figure 1 provides an example of the software output for a patient with an obstructive left anterior descending (LAD) lesion predominantly comprised of NCP and LD-NCP. Figure 2 reflects the AI generated analysis of a non-obstructive LAD lesion comprised of NCP

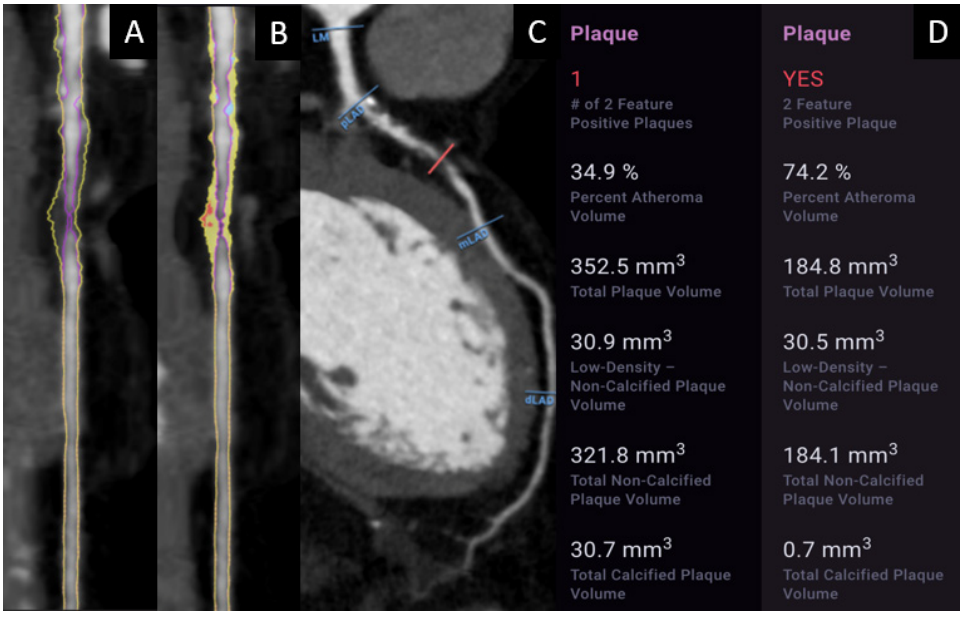

Figure 1 A 39-year-old with coronary CT angiography (CCTA) undergoing artificial intelligence (AI)-aided evaluation of stenosis and quantitative atherosclerosis burden. The patient demonstrates left anterior descending coronary artery obstructive stenosis (82%) with a burden of plaque (352.5 mm^3) consisting predominantly of non-calcified (321.8 mm^3) that includes low-density non-calcified plaque (LD-NCP 30.5 mm^3). (A) shows a CCTA straight reformat with plaque identified, while (B) shows a straight reformat with a colour overlay of non-calcified plaque (yellow), LD-NCP (red) and calcified plaque (blue). (C) shows a curved multiplanar reformat. (D) shows a graphical output of the quantified plaque volume by AI-aided evaluation. dLAD, distal left anterior descending; LM, left main; mLAD, mid left anterior descending; pLAD, proximal left anterior descending.

and LD-NCP while figure 3 provides an example of an right coronary artery (RCA) lesion comprised mostly of calcified plaque.

- Vascular remodelling: Arterial remodelling was calculated by examining the lesion diameter divided by the normal reference diameter. PR was defined as a ratio

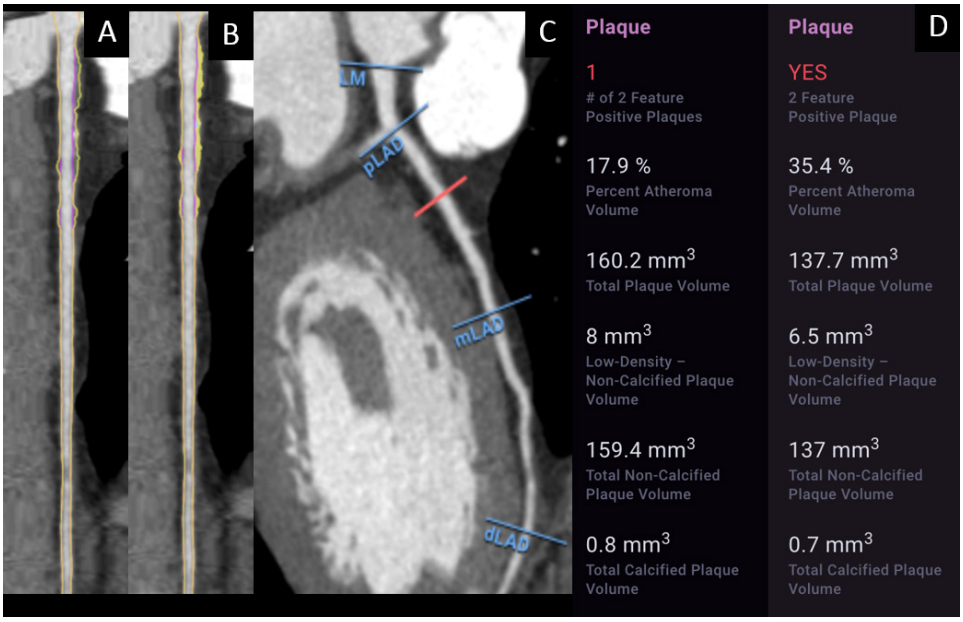

Figure 2 A 55-year-old with coronary CT angiography (CCTA) undergoing artificial intelligence (AI)-aided evaluation of stenosis and quantitative atherosclerosis burden. The patient demonstrates left anterior descending coronary artery non-obstructive stenosis (25%) with a burden of plaque (160.2 mm^3) consisting predominantly of non-calcified (159.4 mm^3) that includes non-negligible low-density non-calcified plaque (8 mm^3). (A) shows a CCTA straight reformat with plaque identified, while (B) shows a straight reformat with a colour overlay of non-calcified plaque (yellow). (C) shows a curved multiplanar reformat. (D) shows a graphical output of the quantified plaque volume by AI-aided evaluation. dLAD, distal left anterior descending; LM, left main; mLAD, mid left anterior descending; pLAD, proximal left anterior descending.

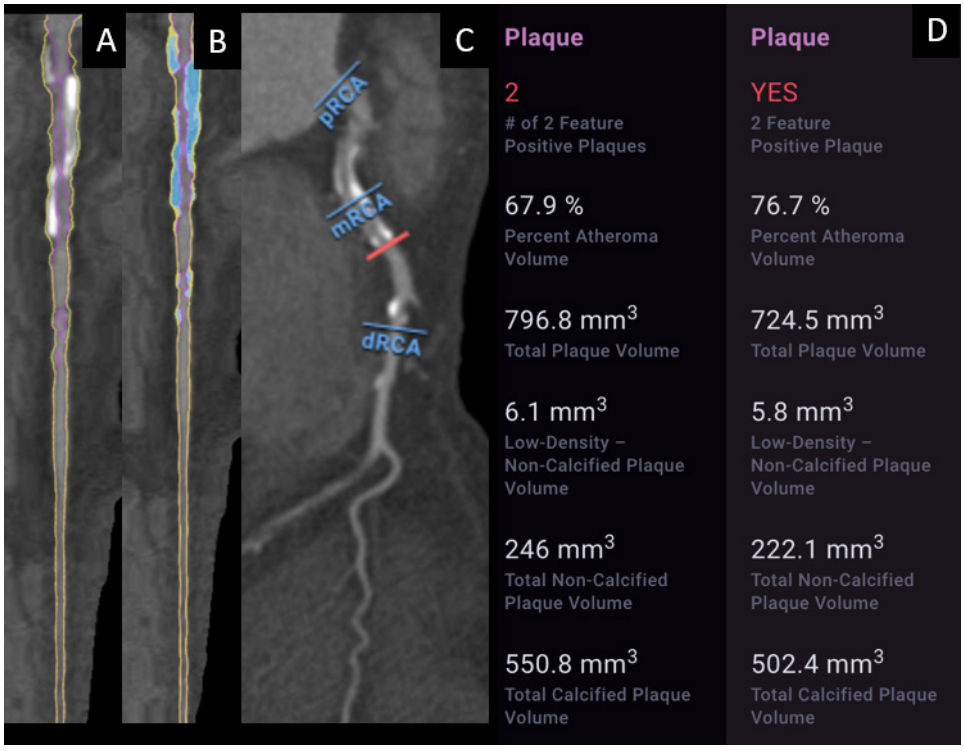

Figure 3 A 74-year-old with coronary CT angiography (CCTA) undergoing artificial intelligence (AI)-aided evaluation of stenosis and quantitative atherosclerosis burden. The patient demonstrates right coronary artery obstructive stenosis (61%) with a high burden of plaque (796.8 mm^3) consisting predominantly of calcified plaque (550.8 mm^3). (A) shows a CCTA straight reformat with plaque identified, while (B) shows a straight reformat with a colour overlay of non-calcified plaque (yellow), and calcified plaque (blue). (C) shows a curved multiplanar reformat. (D) shows a graphical output of the quantified plaque volume by AI-aided evaluation. dLAD, distal left anterior descending; LM, left main; mLAD, mid left anterior descending; pLAD, proximal left anterior descending.

≥1.10, negative remodelling was defined as a ratio of <0.95 and intermediate remodelling was a ratio between 0.95 and 1.10.[15]

- HRP: HRPs were defined as coronary lesions with both LD-NCP and PR.[7]
- Other APCs: Plaque length measured uninterrupted plaque along the length of a vessel. Plaque diffusivity was the percent plaque along the length of a vessel divided by the total vessel length.[16]

Quantitative coronary angiography

Quantitative coronary angiography (QCA) was performed by a blinded core laboratory using an automated edge-detection algorithm by standard approaches as previously reported.[17] Angiographic percent diameter stenosis, and lumen diameters of the proximal and distal reference segments were measured.

Statistical analysis

All statistical analyses were performed using SAS V.9.4 (SAS, Cary, North Carolina). Continuous data are reported as mean±SD, and categorical variables are presented as absolute numbers with corresponding frequencies. Student's t-test, Mann-Whitney test, χ^2 and Fisher exact tests were used to compare the distribution of continuous and categorical variables, respectively.

Patient and public involvement statement

This is a retrospective study that analyses prospectively collected de-identified multicentre data from the CREDENCE trial. Patients were recruited and consented for participation in the CREDENCE trial, but were not interactive with investigators conducting the substudy analysis. However, patients were involved in the design of the study to the extent that their invasive and non-invasive imaging was used to conduct this substudy, and study findings are aimed at improving clinical knowledge of cardiac disease in their cohort.

RESULTS

The study cohort was comprised of 303 patients whose mean age was 64.4±10.2 years. The cohort was 29% women, 71% Asian and had a high prevalence of CAD risk factors including 64% with hypertension, 45% with dyslipidaemia and 48% with prior tobacco use (table 1). Nearly half of the patients (48%) demonstrated typical or atypical angina, while over one-third (35%) were asymptomatic. When stratifying by QCA there were significantly more women with non-obstructive (<50%) CAD (39% vs 22% p=0.001). Patients with obstructive stenosis (≥50%) were significantly more likely than patients with non-obstructive stenosis to have a family history of CAD and to have used tobacco, with

Table 1 Baseline demographics

	All (n=303)	Non-obstructive (<50%) (n=128)	Obstructive (≥50%) (n=175)	P value
Age, years, mean (SD)	64.4 (10.2)	64.3 (10.2)	64.6 (10.2)	0.8
Female	88 (29%)	50 (39%)	38 (22%)	0.001
Hypertension	195 (64%)	79 (62%)	116 (66%)	0.41
Dyslipidaemia	135 (45%)	56 (44%)	79 (45%)	0.81
Diabetes	95 (31%)	38 (30%)	57 (33%)	0.59
Family history	59 (20%)	18 (14%)	41 (23%)	0.04
Tobacco use	146 (48%)	53 (41%)	93 (53%)	0.04
Symptoms				
Typical angina	109 (36%)	36 (28%)	73 (42%)	0.11
Atypical	49 (16%)	23 (18%)	26 (15%)	
Non-cardiac	40 (13%)	19 (15%)	21 (12%)	
Asymptomatic	105 (35%)	50 (39%)	55 (31%)	

no differences noted for prevalence of hypertension, dyslipidaemia or diabetes (table 2). Among younger (age <65) versus older patients (age ≥65), hypertension was more commonly observed in older than younger patients (74% vs 53%). There were no significant differences in gender composition, dyslipidaemia, diabetes or symptoms between younger and older individuals.

Table 3 summarises CCTA findings evaluated by AI as a function of non-obstructive (<50%) and obstructive (≥50%) stenosis by QCA for patients <65 and ≥65 on a per-patient basis. In patients with both non-obstructive (<50%) and obstructive stenosis, patients ≥65 had overall significantly greater plaque volume, total plaque %PAV, and calcified plaque when compared with patients <65. In examining specific APCs, older patients had overall higher PV (792.7±486.1 mm^3 vs 500.1+349.8 mm^3; p<0.0001) across plaque components including higher calcified plaque (366.5±336.2 mm^3 vs 148.0±187.5 mm^3; p<0.0001) and calcified %PAV (4.6% vs 2.6%; p=0.01). However, younger patients with non-obstructive disease demonstrated a similar degree of NCP (243.0±220.2 mm^3 vs 286.5±190.2 mm^3; p=NS) and LD-NCP (8.6±11.1 mm^3 vs 8.9±12.9 mm^3; p=NS) when compared with older patients. Obstructive lesions in patients >65 had higher PAV of calcified (8.1% vs 3.2%; p<0.0001); and NCP (9.1% vs 7.6%; p=0.007) than younger patients with obstructive lesions (table 3).

Further evaluating APCs on an individual lesion basis, table 4 shows the PV by AI-QCT of individual non-obstructive lesions was greater in patients ≥65 versus patients <65 (105.6 mm^3 vs 60.5 mm3; p<0.005). However, non-obstructive lesions in patients <65 exhibit a greater proportion of %PAV (LD-NCP) (1.5% vs 0.7%; p=0.038),

Table 2 Demographics of patients with non-obstructive stenoses and obstructive stenosis by age

				Non-obstructive (<50%) (N=128)			Obstructive (≥50%) (N=175)		
Variable, n (%)	Age <65 (N=139)	Age ≥65 (N=164)	P value	Age <65 (N=62)	Age ≥65 (N=66)	P value	Age <65 (N=77)	Age ≥65 (N=98)	P value
Age, years, mean (SD)	55.7 (7)	71.9 (5)	<0.001	56.1 (7)	71.9 (6)	<0.0001	55.3 (7)	71.8 (5)	<0.0001
Female	36 (26)	52 (32)	0.27	23 (37)	27 (41)	0.66	13 (17)	25 (26)	0.17
Hypertension	74 (53)	121 (74)	<0.0001	33 (53)	46 (70)	0.05	41 (53)	75 (77)	0.001
Dyslipidaemia	56 (40)	79 (48)	0.17	24 (39)	32 (49)	0.26	32 (42)	47 (48)	0.40
Diabetes	38 (27)	57 (35)	0.17	17 (27)	21 (32)	0.59	21 (27)	36 (37)	0.18
Family history	35 (25)	24 (15)	0.02	13 (21)	5 (8)	0.03	22 (29)	19 (19)	0.15
Tobacco use	75 (54)	71 (43)	0.06	26 (42)	27 (41)	0.90	49 (64)	44 (45)	0.01
Symptoms			0.31			0.95			0.06
Typical angina	52 (37)	57 (35)		18 (29)	18 (27)		34 (44)	39 (40)	
Atypical	25 (18)	24 (14)		10 (16)	13 (20)		15 (20)	11 (11)	
Non-cardiac	13 (9)	27 (16)		9 (15)	10 (15)		4 (5)	17 (17)	
Asymptomatic	49 (32)	56 (34)		25 (40)	25 (38)		24 (31)	31 (32)	

Table 3 Per-patient adverse plaque characteristics by artificial intelligence enabled quantitative coronary computed tomographic angiography by non-obstructive versus obstructive angiographic stenosis stratified by age

	Non-obstructive (<50%) per-patient (N=128)			Obstructive (≥50%) per-patient (N=175)		
Variable, mean (SD)	Age <65 (N=62)	Age ≥65 (N=66)	P value	Age <65 (N=77)	Age ≥65 (N=98)	P value
PV, mm^3	357.5 (379.3)	510.7 (206.2)	0.02	500.1 (349.8)	792.7 (486.1)	<0.0001
LD-NCP, mm^3	8.6 (11.1)	8.9 (12.9)	0.46	15.0 (15.3)	12.4 (15.8)	0.11
NCP, mm^3	243.0 (220.2)	286.5 (190.2)	0.10	352.1 (266.8)	426.2 (262.7)	0.02
CP, mm^3	114.5 (190.5)	224.2 (372.1)	0.007	148.0 (187.5)	366.5 (336.2)	<0.0001
Total plaque %PAV	8.2 (7.3)	11.1 (8.6)	0.03	10.7 (6.9)	17.2 (9.7)	<0.0001
LD-NCP %PAV	0.2 (0.2)	0.2 (0.3)	0.41	0.3 (0.3)	0.2 (0.2)	0.07
NCP %PAV	5.6 (4.4)	6.5 (4.0)	0.14	7.6 (5.1)	9.1 (4.7)	0.007
CP %PAV	2.6 (3.6)	4.6 (6.2)	0.01	3.2 ((4.0)	8.1 (7.0)	<0.0001
% plaque calcified	25.3 (21.3)	33.9 (22.4)	0.21	26.6 (21.3)	42.5 (20.5)	<0.0001
Remodelling index	1.30 (0.20)	1.35 (0.21)	0.50	1.38 (0.23)	1.40 (0.22)	0.44
Positive remodelling >1.1, n (%)	48 (79)	55 (83)	0.56	67 (88)	88 (90)	0.73
Intermediate remodelling, n (%)	10 (16)	10 (15)		9 (12)	10 (10)	
Negative remodelling, n (%)	3 (5)	1 (2)		0	0	
HRP (LD-NCP +PR), n (%)	43 (69)	51 (77)	0.31	61 (79)	79 (81)	0.82
Lesion length, mm	23.5 (13.7)	31.9 (21.1)	0.02	28.7 (14.8)	37.6 (19.6)	<0.001

CP, calcified plaque; HRP, high risk plaque; LD-NCP, low-density non-calcified plaque; NCP, non-calcified plaque; %PAV, percent atheroma volume; PR, positive remodelling ; PV, plaque volume.

Table 4 Per-lesion adverse plaque characteristics by artificial intelligence enabled quantitative coronary computed tomographic angiography by non-obstructive versus obstructive angiographic stenosis stratified by age

	Non-obstructive (<50%) per-lesion			Obstructive (≥50%) per-lesion		
Variable	Age <65 (N=71)	Age ≥65 (N=116)	P value	Age <65 (N=77)	Age ≥65 (N=98)	P value
PV, mm^3	60.5 (79.8)	105.6 (140.5)	0.001	103.8 (134.5)	109.7 (131.4)	0.83
LD-NCP, mm^3	1.6 (3.1)	2.0 (6.6)	0.56	4.2 (8.2)	2.6 (10.0)	0.26
NCP, mm^3	38.4 (50.8)	56.2 (75.8)	0.058	74.6 (108.1)	61.5 (85.8)	0.33
CP, mm^3	22.1 (39.1)	49.4 (86.8)	0.004	29.2 (51.5)	48.2 (72.7)	0.04
PAV (total plaque)	41.0 (17.4)	44.8 (16.8)	0.17	49.9 (18.6)	54.7 (16.5)	0.07
% PAV (LD-NCP)	1.5 (3.3)	0.7 (1.3)	0.038	2.0 (3.0)	1.2 (2.8)	0.12
% PAV (NCP)	25.6 (12.4)	25.2 (12.9)	0.81	33.1 (19.3)	30.5 (15.4)	0.32
% PAV (CP)	13.7 (15.7)	18.6 (18.1)	0.07	13.9 (15.6)	30.5 (15.4)	0.001
% Plaque calcified	28.0 (28.5)	36.8 (28.9)	0.06	27.3 (26.8)	38.2 (27.3)	0.007
Remodelling index	1.13 (0.20)	1.06 (0.21)	0.02	1.10 (0.28)	1.05 (0.28)	0.24
Positive remodeling >1.1	29 (41%)	34 (29%)	0.36	25 (33%)	29 (30%)	0.78
Intermediate remodelling	28 (39%)	46 (40%)		26 (34%)	27 (28%)	
Negative remodelling	14 (20%)	36 (31%)		26 (34%)	42 (43%)	
HRP (LD-NCP +PR)	34 (48%)	42 (36%)	0.16	31 (40%)	33 (34%)	0.40
Lesion length, mm	13.9 (10.4)	18.1 (15.6)	0.02	18.3 (15.5)	18.2 (15.1)	0.90

CP, calcified plaque; HRP, high risk plaque; LD-NCP, low-density non-calcified plaque; NCP, non-calcified plaque; PAV, per cent atheroma volume; PR, positive remodelling ; PV, plaque volume.

near significantly higher volume of NCP in age <65 (38.4 mm^3 vs 56.2 mm3; p<0.058), as well as a higher remodelling index (1.13 vs 1.06; p=0.02) with shorter lesion length (13.9 mm vs 18.1 mm; p=0.02). An illustrative case of obstructive stenosis in a 39-year-old with high NCP and LD-NCP burden is shown in figure 1. An illustrative case of non-obstructive stenosis in a 55-year-old with high NCP is shown in figure 2. Age >65 patients with non-obstructive lesions exhibit higher calcified plaque (49.4 mm^3 vs 22.1 mm^3; p=0.004) and near significant % plaque calcified (36.8% vs 28.0%; p=0.06) compared with patient <65. An illustrative case of calcified plaque in a 74-year-old with high calcified burden is shown in figure 3.

Online supplemental appendix C shows per-patient and per-lesion analysis within the younger and older age cohorts for non-obstructive and obstructive stenoses. In both younger and older individuals, PV and CP are higher for obstructive stenosis versus non-obstructive stenosis. In older adults, there was no difference between the volume of LD-NCP in non-obstructive and obstructive lesions, while calcified plaque was significantly higher in obstructive versus non-obstructive lesions (366.5 mm^3 vs 224 mm^3; p=0.01).

DISCUSSION

In this analysis of CREDENCE, we uniquely applied AI for quantitative plaque evaluation and add several important new observations to the expanding body of literature on APC identified by CCTA. Our study found that APCs of high-grade stenoses differ by age with patients <65 years exhibiting greater PV, LD-NCP, NCP and lesion length in obstructive lesions compared with non-obstructive lesions. Patients >65 years exhibited a greater burden of calcified plaque in both non-obstructive and obstructive stenoses. Furthermore, in patients >65 with obstructive stenosis, while there was a higher calcified and NCP burden, younger patients had similar LD-NCP as older patients with obstructive lesions.

Recent validation of the AI-guided approach applied in this study allows for accurate AI evaluation of stenosis as well allowing for quantification of PV to an order of 3–5 mm^3 that may not be readily identified by expert readers.[12 18 19] This data extends atherosclerosis evaluation beyond previous logistic regression models incorporating plaque as one of many variables defined by manual methods.[20] In addition, the use of well-validated deep machine learning approaches allows for enhanced and rapid image processing. Previous validation data from our group has shown that this AI approach can perform whole heart atherosclerosis and stenosis evaluation in approximately 10 min, whereas manual approaches may take several hours to complete and be prone to variability.

Through this AI approach, we show that atherosclerosis in younger adults with non-obstructive stenoses demonstrate comparable plaque characterisation when compared with older adults. This includes the presence of high-risk plaque features such as NCP, LD-NCP and PR that qualitatively portend, by SCCT expert consensus, a future risk of cardiovascular events.[21] Importantly, AI identified a higher PAV of LD-NCP in younger individuals with non-obstructive atherosclerosis, a plaque type identified as highest risk by cardiac CT.[22] These data affirm prior findings that younger patients have high volumes of non-calcified atherosclerosis with a higher degree of LD-NCP, while older patients develop a higher degree of calcified plaque in both non-obstructive and obstructive lesions.[22] Lowenstern *et al*'s subanalysis of the PROMISE (Prospective Multicenter Imaging Study for Evaluation of Chest Pain) study also supports the finding that older patients have more calcified plaque.[23] However, importantly, the study also showed that high calcium scores did not confer risk for MACE in older patients while it did conferred risk for MACE in individuals younger than 65.[23] The study does not comment on additional APCs like LD-NCP, but remains consistent with our findings and re-emphasises the benefit of addressing plaque characteristics for prognostication for MACE at different ages. In our study, age stratification identified differences in overall plaque burden, which may help identify younger patients who may be at risk for future acute coronary syndrome (ACS) despite having non-obstructive stenoses.

While the literature on APCs and high-risk lesion assessment is rapidly expanding, there is still limited information regarding age-oriented plaque composition. In particular, identifying which younger adults are at risk for CAD remains challenging due to limitations in current risk calculators and insufficient data in this group.[24] Additionally, limitations exist in identifying atherosclerosis via conventional approaches, such as stress testing, making younger adults less likely to be treated with preventive therapies. While Ruiz-García *et al* published a substudy of the PROSPECT (Prospective Natural History Study of Coronary Atherosclerosis) trial evaluating APCs of non-culprit lesions via intravascular ultrasound (IVUS) that concluded that patients older than 65 had greater plaque burden, necrotic core and dense calcium content than patients younger than 65 (regardless of gender),[25] this study involved non-culprit lesions in patients who had already experienced ACS and could not be generalised to a younger population in the preventive stages of disease.

In the CCTA literature, an age-based study was recently conducted by Conte *et al* who evaluated a subgroup of patients from the ICONIC (Incident Coronary Syndromes Identified by Computed Tomography) trial to determine whether APCs of culprit lesions varied by age and showed that older patients had greater total PV, specifically calcified plaque, as well as greater segment involvement and segment severity scores than younger patients.[26] However, again, the study cohort was comprised of ACS patients and the lesion level analysis pertained specifically to culprit lesions, limiting the ability to generalise findings. Additionally, Kim *et al* initiated a substudy of the PARADIGM (Progression of AtheRosclerotic PlAque DetermIned by Computed TomoGraphic Angiography Imaging) trial, a cohort with suspected or known CAD, and showed that

the rate of plaque progression, specifically densely calcified plaque, increased with age.[27] The study's intention was to identify gross trends in a middle-aged cohort (40–75 years), and to that end, whole heart plaque was evaluated while lesion-based changes were unaddressed.

While calcified plaque increases with age, a finding consistent with our data, this does not account for the high risk ACPs at younger ages that may be important for early screening.[24 28] Our study findings suggest that the quantification of APCs associated within plaque identified by AI-QCT, namely, LD-NCP, NCP and PV and lesion length may also provide prognostic value when screening patients <65 years. Understanding this plaque phenotype also may allow for enhanced opportunities to understand and modulate the plaque phenotype through preventive therapies such as statins and newer agents such as PCSK-9 inhibition.[29]

This study is subject to limitations. While patients were enrolled prospectively from a large, multicentre clinical trial with evaluation by a blinded core laboratory, the evaluation was post hoc and not powered to detect differences in plaque types. About one-third of the patients had demonstrable atherosclerosis despite the absence of symptoms, which may not be fully representative of a stable chest pain population, but also represent a limitation in current guidelines for testing. Additionally, the CCTAs evaluated reflect a single point in time rather than a longitudinal period thereby limiting knowledge of plaque progression as reflected at various ages. Though coronary lesions are dynamic, changes in PV composition as a function of worsening stenosis severity was not evaluated. Finally, we used angiographic coronary stenosis as a marker of CAD severity. While large-scale prognosis of AI-QCT defined quantitative plaque composition has not yet been performed, it remains the subject of future study in the upcoming CONFIRM2 study (Coronary CT Angiography Evaluation for Clinical Outcomes: An International Multicenter Registry; NCT04279496).

In sum, AI-QCT identifies a unique APC signature that differs by age with patients <65 years exhibiting greater PV, LD-NCP, NCP and lesion length in obstructive compared with non-obstructive lesions. While no difference in plaque composition was observed in obstructive stenoses for patients >65 years, older patients had greater CP volume and patients <65 had more NCP and LD-NCP. These findings have important implications for prognosticating younger and older adults with unique plaque phenotypes identified by AI-QCT that allows a foundation for AI-guided precision approaches to cardiovascular prevention.

Author affiliations
[1]Thomas Jefferson University Hospital, Philadelphia, Pennsylvania, USA
[2]Cleerly Health, New York, New York, USA
[3]UNICA, Unit of Cardiovascular Imaging, CHRC Campus Nova Medical School, Lisboa, Portugal
[4]Cardiology, Yonsei University Health System, Seodaemun-gu, Seoul, Korea
[5]Ontact Health, Inc, Seoul, Korea
[6]Department of Medicine, Inje University Ilsan Paik Hospital, Goyang, Korea
[7]Cardiology, Kangwon National University Hospital, Chuncheon, Kangwon, Korea
[8]Department of Internal Medicine, Seoul National University Hospital, Jongno-gu, Seoul, Korea
[9]Cardiovascular Center, Keimyung University Dongsan Hospital, Daegu, Korea
[10]Division of Cardiology, Department of Internal Medicine, Catholic Kwandong University International Saint Mary's Hospital, Incheon, Korea (the Republic of)
[11]Cardiology, Ewha Women's University Mokdong Hospital, Seoul, Korea
[12]Mobile Cardiology Associates, Mobile, Alabama, USA
[13]Department of Imaging, Fondazione Toscana Gabriele Monasterio, Pisa, Italy
[14]Cardiac Center of Texas, McKinney, Texas, USA
[15]Department of Radiology, Fuwai Hospital State Key Laboratory of Cardiovascular Disease, Beijing, China
[16]Fuwai Hospital State Key Laboratory of Cardiovascular Disease, Beijing, China
[17]Houston Methodist Hospital, Houston, Texas, USA
[18]Cardiovascular Center, Saint Luke's International Hospital, Chuo-ku, Tokyo, Japan
[19]Department of Radiology and Radiological Science, Medical University of South Carolina, Charleston, South Carolina, USA
[20]VU University Medical Centre Amsterdam, Amsterdam, Noord-Holland, Netherlands
[21]Department of Cardiology, Vrije Universiteit Amsterdam, Amsterdam, Netherlands
[22]Saint Luke's Mid America Heart Institute, Kansas City, Missouri, USA
[23]Cardiology, Kaiser Permanente, San Jose, California, USA
[24]Heart Center Research, Huntsville, Alabama, USA
[25]Renown Health, Reno, Nevada, USA
[26]Oconee Heart and Vascular Center, Saint Marys Medical Group, Athens, Georgia, USA
[27]Division of Cardiology, Hopital du Sacre-Coeur de Montreal, Montreal, Québec, Canada
[28]Cardiology, VU University Medical Centre Amsterdam, Amsterdam, Noord-Holland, Netherlands
[29]Centro Cardiologico Monzino Istituto di Ricovero e Cura a Carattere Scientifico, Milano, Lombardia, Italy
[30]Cardiology, Houston Methodist Hospital, Houston, Texas, USA
[31]Medicine (Cardiology), University of Virginia Health System, Charlottesville, Virginia, USA
[32]Division of Cardiology and Department of Radiology, The George Washington University School of Medicine and Health Sciences, Washington, District of Columbia, USA

Twitter Andrew D Choi @AChoiHeart

Contributors JE, RJe and JKM contributed to blinded core imaging core laboratory analysis and statistical support as requested by the study authors. RJo, ADC and TRC evaluated statistical methodology. RJo, JPE (prior to employment by Cleerly) and ADC conceived and designed the analysis, performed the analysis, wrote the paper and evaluated methodology. All other authors provided acquisition of study data as well as critical revision of the manuscript for important intellectual content. This study was an investigator initiated study.

Funding ADC is supported by a grant from the GW Heart and Vascular Institute.

Competing interests Equity Interest Cleerly, JE, HM, ADC, Employees of Cleerly – RJe, TRC, JKM, JE.

Patient consent for publication Not applicable.

Ethics approval The institutional review board of each enrolling site approved the study protocol and all patients provided written informed consent.

Provenance and peer review Not commissioned; internally peer reviewed.

Data availability statement Data may be obtained from a third party and are not publicly available. Index data for the CREDENCE trial has been previously published. De-identified patient data are not publicly available, except if necessary to confirm study results; requests for data may be made by contacting Dr James Min (James.Min@cleerlyhealth.com).

ORCID iDs
Rebecca Jonas http://orcid.org/0000-0003-0203-6210

Guus A de Waard http://orcid.org/0000-0003-0813-7725

REFERENCES

1 Marwick TH, Cho I, Ó Hartaigh B, *et al*. Finding the gatekeeper to the cardiac catheterization laboratory: coronary CT angiography or stress testing? *J Am Coll Cardiol* 2015;65:2747–56.
2 Budoff MJ, Dowe D, Jollis JG, *et al*. Diagnostic performance of 64-multidetector row coronary computed tomographic angiography for evaluation of coronary artery stenosis in individuals without known coronary artery disease: results from the prospective multicenter accuracy (assessment by coronary computed tomographic angiography of individuals undergoing invasive coronary angiography) trial. *J Am Coll Cardiol* 2008;52:1724–32.
3 Abdelrahman KM, Chen MY, Dey AK, *et al*. Coronary computed tomography angiography from clinical uses to emerging technologies: JACC state-of-the-art review. *J Am Coll Cardiol* 2020;76:1226–43.
4 Singh G, Al'Aref SJ, Van Assen M, *et al*. Machine learning in cardiac CT: basic concepts and contemporary data. *J Cardiovasc Comput Tomogr* 2018;12:192–201.
5 Puchner SB, Liu T, Mayrhofer T, *et al*. High-risk plaque detected on coronary CT angiography predicts acute coronary syndromes independent of significant stenosis in acute chest pain: results from the ROMICAT-II trial. *J Am Coll Cardiol* 2014;64:684–92.
6 Diaz-Zamudio M, Fuchs TA, Slomka P, *et al*. Quantitative plaque features from coronary computed tomography angiography to identify regional ischemia by myocardial perfusion imaging. *Eur Heart J Cardiovasc Imaging* 2017;18:499–507.
7 Stuijfzand WJ, van Rosendael AR, Lin FY, *et al*. Stress myocardial perfusion imaging vs coronary computed tomographic angiography for diagnosis of invasive Vessel-Specific coronary physiology: predictive modeling results from the computed tomographic evaluation of atherosclerotic determinants of myocardial ischemia (CREDENCE) trial. *JAMA Cardiol* 2020;5:1338–48.
8 Nerlekar N, Ha FJ, Cheshire C, *et al*. Computed tomographic coronary Angiography-Derived plaque characteristics predict major adverse cardiovascular events: a systematic review and meta-analysis. *Circ Cardiovasc Imaging* 2018;11:e006973.
9 Feuchtner G, Kerber J, Burghard P, *et al*. The high-risk criteria low-attenuation plaque <60 HU and the napkin-ring sign are the most powerful predictors of MACE: a long-term follow-up study. *Eur Heart J Cardiovasc Imaging* 2017;18:772–9.
10 Rizvi A, Hartaigh Bríain Ó, Knaapen P, *et al*. Rationale and design of the CREDENCE trial: computed tomographic evaluation of atherosclerotic determinants of myocardial ischemia. *BMC Cardiovasc Disord* 2016;16:190.
11 Abbara S, Blanke P, Maroules CD, *et al*. SCCT guidelines for the performance and acquisition of coronary computed tomographic angiography: a report of the Society of Cardiovascular Computed Tomography Guidelines Committee: endorsed by the North American Society for Cardiovascular Imaging (NASCI). *J Cardiovasc Comput Tomogr* 2016;10:435–49.
12 United States Food and Drug Administration. Cleerly Labs 510 (K) premarket notification, 2019. Available: https://www.accessdata.fda.gov/cdrh_docs/pdf19/K190868.pdf
13 Choi AD, Marques H, Kumar V. CT evaluation by artificial intelligence for atherosclerosis, stenosis and vascular morphology (CLARIFY): a multi-center, international study. *J Cardiovasc Comput Tomogr* 2021;15:470–6.
14 Leipsic J, Abbara S, Achenbach S, *et al*. SCCT guidelines for the interpretation and reporting of coronary CT angiography: a report of the Society of cardiovascular computed tomography guidelines Committee. *J Cardiovasc Comput Tomogr* 2014;8:342–58.
15 Nakazato R, Shalev A, Doh J-H, *et al*. Quantification and characterisation of coronary artery plaque volume and adverse plaque features by coronary computed tomographic angiography: a direct comparison to intravascular ultrasound. *Eur Radiol* 2013;23:2109–17.
16 Rizvi A, Hartaigh Bríain Ó, Danad I, *et al*. Diffuse coronary artery disease among other atherosclerotic plaque characteristics by coronary computed tomography angiography for predicting coronary vessel-specific ischemia by fractional flow reserve. *Atherosclerosis* 2017;258:145–51.
17 Danad I, Raijmakers PG, Driessen RS, *et al*. Comparison of coronary CT angiography, SPECT, PET, and hybrid imaging for diagnosis of ischemic heart disease determined by fractional flow reserve. *JAMA Cardiol* 2017;2:1100–7.
18 Choi AD, Marques H, Kumar V, *et al*. CT evaluation by artificial intelligence for atherosclerosis, stenosis and vascular morphology (clarify): a multi-center, internaltional study. *J Cardiovasc Comput Tomogr* 2021.
19 Choi AD, Blankstein R. Becoming an expert practitioner: the lifelong journey of education in cardiovascular imaging. *JACC Cardiovasc Imaging* 2021;14:1594–7.
20 Al'Aref SJ, Maliakal G, Singh G, *et al*. Machine learning of clinical variables and coronary artery calcium scoring for the prediction of obstructive coronary artery disease on coronary computed tomography angiography: analysis from the CONFIRM registry. *Eur Heart J* 2020;41:359–67.
21 Shaw LJ, Blankstein R, Bax JJ, *et al*. Society of Cardiovascular Computed Tomography / North American Society of Cardiovascular Imaging - Expert Consensus Document on Coronary CT Imaging of Atherosclerotic Plaque. *J Cardiovasc Comput Tomogr* 2021;15:93–109.
22 Schmermund A, Schwartz RS, Adamzik M, *et al*. Coronary atherosclerosis in unheralded sudden coronary death under age 50: histo-pathologic comparison with 'healthy' subjects dying out of hospital. *Atherosclerosis* 2001;155:499–508.
23 Lowenstern A, Alexander KP, Hill CL, *et al*. Age-related differences in the noninvasive evaluation for possible coronary artery disease: insights from the prospective multicenter imaging study for evaluation of chest pain (PROMISE) trial. *JAMA Cardiol* 2020;5:193–201.
24 Michos ED, Choi AD. Coronary artery disease in young adults: a hard lesson but a good teacher. *J Am Coll Cardiol* 2019;74:1879–82.
25 Ruiz-García J, Lerman A, Weisz G, *et al*. Age- and gender-related changes in plaque composition in patients with acute coronary syndrome: the PROSPECT study. *EuroIntervention* 2012;8:929–38.
26 Conte E, Dwivedi A, Mushtaq S, *et al*. Age- and sex-related features of atherosclerosis from coronary computed tomography angiography in patients prior to acute coronary syndrome: results from the ICONIC study. *Eur Heart J Cardiovasc Imaging* 2021;22:24–33.
27 Kim M, Lee S-P, Kwak S, *et al*. Impact of age on coronary artery plaque progression and clinical outcome: a paradigm substudy. *J Cardiovasc Comput Tomogr* 2021;15:232–9.
28 Singh A, Collins BL, Gupta A, *et al*. Cardiovascular Risk and Statin Eligibility of Young Adults After an MI: Partners YOUNG-MI Registry. *J Am Coll Cardiol* 2018;71:292–302.
29 Lee S-E, Chang H-J, Sung JM, *et al*. Effects of Statins on Coronary Atherosclerotic Plaques: The PARADIGM Study. *JACC Cardiovasc Imaging* 2018;11:1475–84.

Appendix A. Participating Sites and Enrolling Investigators

Investigator: Hugo Marques, MD

Nova Medical School - Faculdade de Ciências Médicas,
Lisboa, Portugal

Investigator: Hyuk-Jae Chang, MD PhD[3]

Severance Cardiovascular Hospital and Severance Biomedical Science Institute,
Yonsei University College of Medicine, Yonsei University Health System
Seoul, South Korea

Investigator: Jung Hyun Choi, MD PhD

Pusan National University Hospital
Busan, South Korea

Investigator: Joon-Hyung Doh, MD

University Ilsan Paik Hospital
Goyang, South Korea

Investigator: Ae-Young Her, MD

Kang Won National University Hospital
Chuncheon, South Korea

Investigator: Bon-Kwon Koo, MD PhD

Seoul National University Hospital
Seoul, South Korea

Investigator: Chang-Wook Nam, MD PhD

Keimyung University Dongsan Hospital
Daegu, South Korea

Investigator: Hyung-Bok Park, MD

International St. Mary's Hospital
Catholic Kwandong University College of Medicine
Incheon, South Korea

Investigator: Sang-Hoon Shin, MD

Ewha Women’s University Seoul Hospital

Seoul, South Korea

Investigator: Jason Cole, MD

Mobile Cardiology Associates
Mobile, Alabama, USA

Investigator: Alessia Gimelli, MD

Fondazione Toscana Gabriele Monasterio
Pisa, Italy

Investigator: Muhammad Akram Khan, MD

Cardiac Center of Texas
McKinney, Texas, USA

Investigator: Bin Lu, MD, Yang Gao, MD

State Key Laboratory of Cardiovascular Disease
Fuwai Hospital
Beijing, China

Investigator: Faisal Nabi, MD

Houston Methodist Hospital
Houston, Texas, USA

Investigators: Ryo Nakazato, MD

St. Luke's International Hospital
Tokyo, Japan

Investigator: U. Joseph Schoepf, MD

Medical University of South Carolina
Charleston, SC, USA

Investigators: Roel S. Driessen, MD, Michiel J. Bom, MD, Paul Knaapen, MD, PhD, Guus A. de Waard, MD

Amsterdam University Medical Center
VU University Medical Center
Amsterdam, the Netherlands

Investigator: Randall Thompson, MD

St. Luke's Mid America Heart Institute

Kansas City, MO, USA

Investigator: James J. Jang, MD

Kaiser Permanente Hospital
Oakland, CA, USA

Investigator: Michael Ridner, MD

Heart Center Research, LLC
Huntsville, Alabama, USA

Investigator: Chris Rowan, MD

Renown Heart and Vascular Institute
Reno, NV, USA

Investigator: Erick Avelar, MD

Oconee Heart and Vascular Center at St Mary's Hospital
Athens, GA, USA

Investigator: Philippe Généreux, MD

Gagnon Cardiovascular Institute
Morristown Medical Center
Morristown, NJ, USA

Investigators: Gianluca Pontone, MD, PhD & Daniele Andreini, MD, PhD

Centro Cardiologico Monzino, IRCCS
Milan, Italy

Appendix B: Artificial Intelligence/Machine Learning Steps to CCTA Image Evaluation: The following figures present in graphical detail the stepwise use of artificial intelligence algorithms used for CCTA analysis.

This is an AI-aided approach (Cleerly Inc, New York, NY) that performs an automated analysis of CCTA using a series of validated convolutional neural network models (including VGG 19 network, 3D U-Net and VGG Network Variant) for image quality assessment, coronary segmentation and labeling, lumen wall evaluation and vessel contour determination and plaque characterization(19). No manual interaction is required from the reader. First, the AI-aided approach leverages 2 deep convolutional neural networks (VGG-19 Network and 3D U-Net) to produce a centerline along the length of the vessel, and then for lumen and outer vessel wall contouring. This approach is applied to multiple phases/series of the CCTA examination, if present, and enables phase-specific evaluation at the coronary segment vessel. The algorithm reviewed all series and determined the top 2 optimal series for further analysis including vessel and lumen segmentation, plaque, and stenosis quantification. The algorithm rank-orders all available phases for the segmentation of the arteries. It then uses the top two phases interactively on a per vessel basis, e.g., the right coronary artery (RCA) will be reconstructed from the phase which yields the highest RCA image quality, while the posterior descending artery (PDA) may come from the second phase if the PDA has a higher image quality on that phase. Once coronary artery segmentation is performed, an automated labeling is done to classify arteries by their location as well the proximal, mid and distal portions within a single vessel. The AI further allows for defining of coronary artery lesions (i.e., those areas where plaque is present; VGG Network Variant). Utilizing a normal proximal reference vessel cross-sectional slide, the start and the end of the lesion, and the cross-sectional slice that demonstrates the greatest absolute narrowing, % diameter stenosis severity is automatically calculated. The software determines the start and end of lesions and drops stenosis markers at the region of the highest stenosis. Within coronary artery lesions, plaque is quantified in a similar fashion, and further characterized as low-attenuation non-calcified plaque, non-calcified plaque and calcified plaque based upon Hounsfield unit (HU) densities of <30, -189 to 350, >350, respectively. Positive arterial remodeling was identified as a remodeling index $\geq$1.10 by diameter when compared to a proximal vessel reference. Vessel length, vessel volume, lumen volume, total plaque volume, calcified plaque volume, noncalcified plaque volume, low density noncalcified plaque volume, maximum diameter and area stenosis, and maximum remodeling index are calculated.

Training and testing were performed on a proprietary database. The centerline algorithm was developed from 1,007,945 images, which comprised 23,068 vessels from 3,671 patients. The lumen and vessel wall algorithms were developed from 1,414,877 images, which comprised 8,555 vessels from 3,676 patients.

Information and documentation of U.S. Food and Drug Administration (FDA) approval may additionally be found here in the FDA Access document here:

(https://www.accessdata.fda.gov/cdrh_docs/pdf19/K190868.pdf).

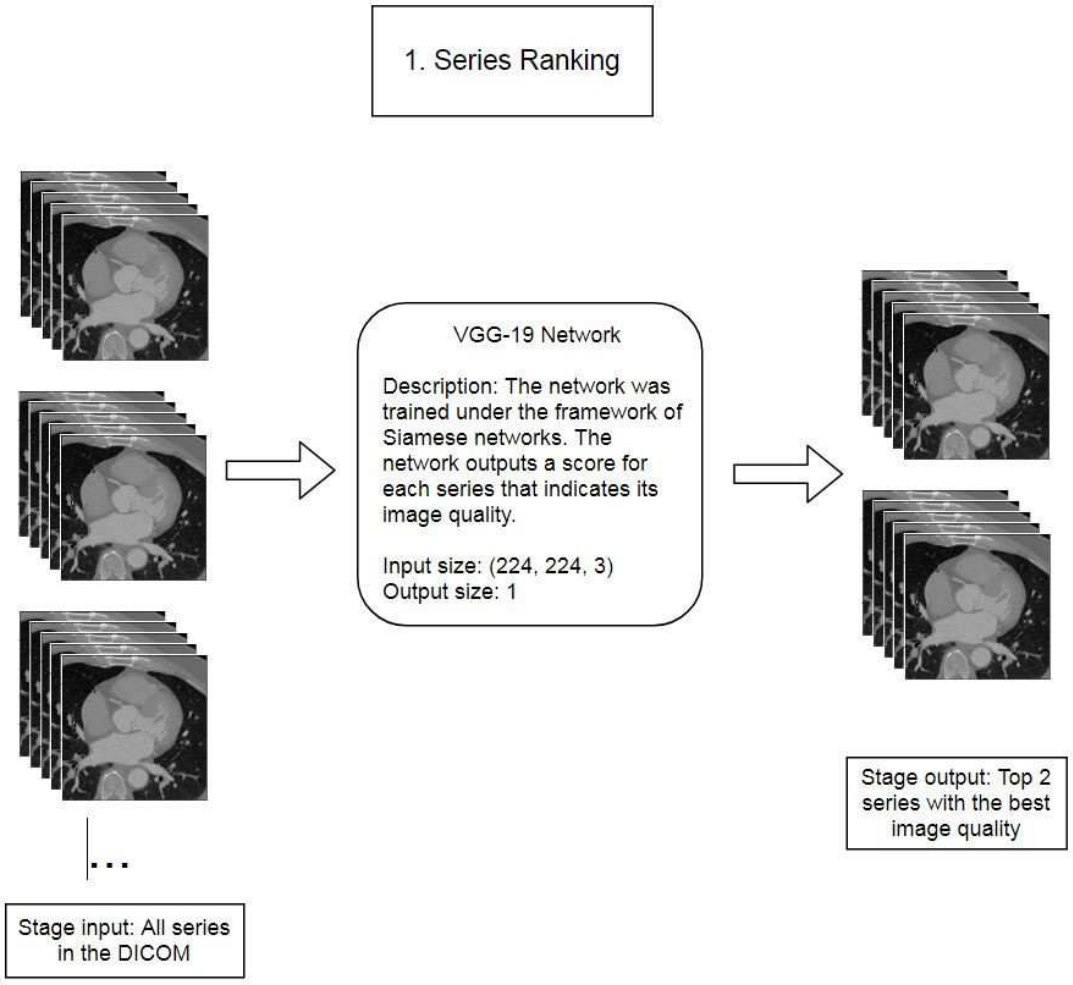
1. Series Ranking
VGG-19 Network
Description: The network was trained under the framework of Siamese networks. The network outputs a score for each series that indicates its image quality.
Input size: (224, 224, 3)
Output size: 1
Stage input: All series in the DICOM
Stage output: Top 2 series with the best image quality

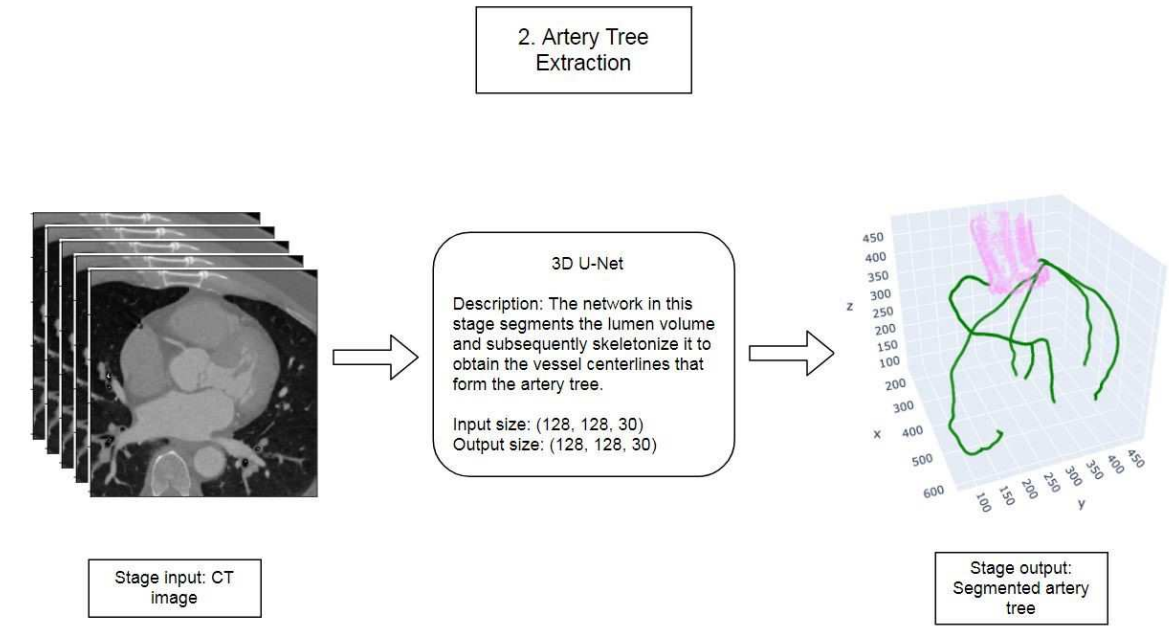
2. Artery Tree Extraction
3D U-Net
Description: The network in this stage segments the lumen volume and subsequently skeletonize it to obtain the vessel centerlines that form the artery tree.
Input size: (128, 128, 30)
Output size: (128, 128, 30)
Stage input: CT image
Stage output: Segmented artery tree

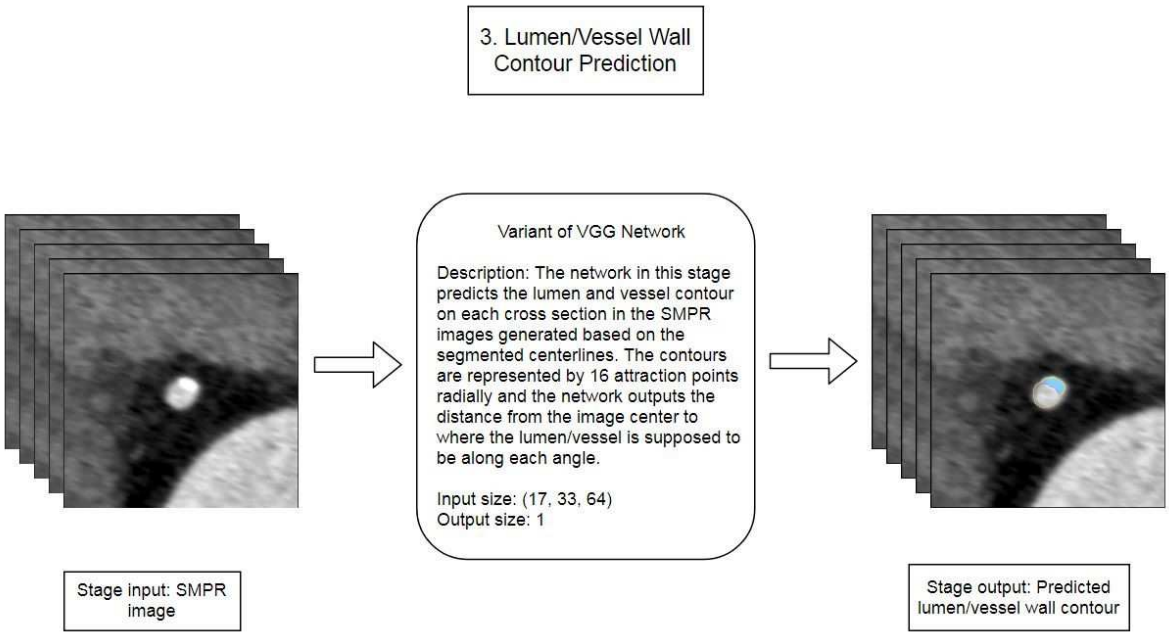
3. Lumen/Vessel Wall Contour Prediction
Variant of VGG Network
Description: The network in this stage predicts the lumen and vessel contour on each cross section in the SMPR images generated based on the segmented centerlines. The contours are represented by 16 attraction points radially and the network outputs the distance from the image center to where the lumen/vessel is supposed to be along each angle.
Input size: (17, 33, 64)
Output size: 1
Stage input: SMPR image
Stage output: Predicted lumen/vessel wall contour

APPENDIX C

Per-Patient and Per-Lesion APCs by for Non-Obstructive vs Obstructive Plaque in Age < 65 and Age ≥ 65 CCTA, Angiographic Stenosis

	Age <65			Age ≥65		
Variable Per Patient, mean (SD)	**Non-obstructive (<50%) (N=62)**	**Obstructive (≥50%) (N=77)**	***P*-Value**	**Non-obstructive (<50%) (N=66)**	**Obstructive (≥50%) (N=98)**	***P*-Value**
PV, mm^3	357.5 (379.3)	500.1 (349.8)	0.00229	510.7 (206.2)	792.7 (486.1)	0.0004
LD-NCP, mm^3	8.6 (11.1)	15.0 (15.3)	0.0046	8.9 (12.9)	12.4 (15.8)	0.14
NCP, mm^3	243.0 (220.2)	352.1 (266.8)	0.0107	286.5 (190.2)	426.2 (262.7)	0.0001
CP, mm^3	114.5 (190.5)	148.0 (187.5)	0.30	224.2 (372.1)	366.5 (336.2)	0.01
% Plaque Calcified	25.3 (21.3)	26.6 (21.3)	0.56	33.9 (22.4)	42.5 (20.5)	0.01
Remodeling Index	1.30 (0.20)	1.38 (0.23)	0.04	1.35 (0.21)	1.40 (0.22)	0.14
Positive Remodeling >1.1, n (%)	48 (79%)	67 (88.2%)	0.09	55 (83%)	88 (90%)	0.29
Intermediate Remodeling, n(%)	10 (16%)	9 (12%)		10 (15%)	10 (10%)	
Negative Remodeling, n (%)	3 (5%)	0		1 (2%)	0	
HRP (LD-NCP+PR), n(%)	43 (69%)	61 (79%)	0.18	51 (77%)	79 (81%)	0.60
Lesion Length, mm	23.5 (13.7)	28.7 (14.8)	0.03	31.9 (21.1)	37.6 (19.6)	0.07
Variable Per Lesion	**Non-obstructive (<50%) (N=71)**	**Obstructive (≥50%) (N=77)**	***P*-Value**	**Non-obstructive (<50%) (N=116)**	**Obstructive (≥50%) (N=98)**	***P*-Value**
Plaque volume, mm^3	60.5 (79.8)	103.8 (134.5)	0.01	105.6 (140.5)	109.7 (131.4)	0.81
LD-NCP, mm^3	1.6 (3.1)	4.2 (8.2)	0.01	2.0 (6.6)	2.6 (10.0)	0.60
NCP, mm^3	38.4 (50.8)	74.6 (108.1)	0.0036	56.2 (75.8)	61.5 (85.8)	0.51
CP, mm^3	22.1 (39.1)	29.2 (51.5)	0.69	49.4 (86.8)	48.2 (72.7)	0.87
Remodeling Index	1.13 (0.20)	1.10 (0.28)	0.15	1.06 (0.21)	1.05 (0.28)	0.71
Positive Remodeling >1.1, n(%)	29 (41%)	25 (33%)	0.15	34 (29%)	29 (30%)	0.11
Intermediate Remodeling, n(%)	28 (39%)	26 (34%)		46 (40%)	27 (28%)	
Negative Remodeling, n(%)	14 (20%)	26 (34%)		36 (31%)	42 (43%)	
HRP (LD-NCP+PR), n(%)	34 (48%)	31 (40%)	0.38	42 (36%)	33 (34%)	0.67
Lesion Length, mm	13.9 (10.4)	18.3 (15.5)	0.03	18.1 (15.6)	18.2 (15.1)	0.96

Abbreviations: PV = plaque volume; PAV = percent atheroma volume; LD-NCP = low-density non-calcified plaque; NCP = non-calcified plaque; CP = calcified plaque; PR = positive remodeling; HRP = High-risk plaque